Endocrinology. First published ahead of print May 31, 2012 as doi:10.1210/en.2012-1107

IGF-I Regulates Pheochromocytoma Cell Proliferation and Survival *In Vitro* and *In Vivo*

María Celia Fernández, Marcela Venara, Susana Nowicki, Héctor E. Chemes,* Marta Barontini,* and Patricia A. Pennisi

Centro de Investigaciones Endocrinológicas Consejo Nacional de Investigaciones Científicas y Técnicas, Hospital de Niños Dr. Ricardo Gutiérrez, C1425EFD Buenos Aires, Argentina

IGFs are involved in malignant transformation and growth of several tissues, including the adrenal medulla. The present study was designed to evaluate the impact of IGF-I on pheochromocytoma development. We used a murine pheochromocytoma (MPC) cell line (MPC4/30) and an animal model with a reduction of 75% in circulating IGF-I levels [liver-IGF-I-deficient (LID) mice] to perform studies *in vitro* and *in vivo*. We found that, in culture, IGF-I stimulation increases proliferation, migration, and anchorage-independent growth, whereas it inhibits apoptosis of MPC cells. When injected to control and to LID mice, MPC cells grow and form tumors with features of pheochromocytoma. Six weeks after cell inoculation, all control mice developed sc tumors. In contrast, in 73% of LID mice, tumor development was delayed to 7–12 wk, and the remaining 27% did not develop tumors up to 12 wk after inoculation. LID mice harboring MPC cells and treated with recombinant human IGF-I (LID+) developed tumors as controls. Tumors developed in control, LID, and LID+ mice had similar histology and were similarly positive for IGF-I receptor expression. The apoptotic index was higher in tumors from LID mice compared with those from control mice, whereas vascular density was decreased. In summary, our work demonstrates that IGF-I has a critical role in maintaining tumor phenotype and survival of already transformed pheochromocytoma cells and is required for the initial establishment of these tumors, providing encouragement to carry on research studies to address the IGF-I/IGF-I receptor system as a target of therapeutic strategies for pheochromocytoma treatment in the future. **(*Endocrinology* 153: 0000–0000, 2012)**

The IGFs are polypeptides structurally related to insulin that play an important role on cellular proliferation and inhibition of apoptosis (1).

IGF-I and IGF-II are synthesized by almost all tissues and are important mediators of cell growth, differentiation, and transformation. They can play a paracrine and/or autocrine role in promoting tumor growth *in situ* during tumor progression. Increased expression of IGF-I, IGF-II, or IGF-I receptor (IGF-IR) have been documented in several malignancies, including glioblastomas, neuroblastomas, meningiomas, medulloblastomas, breast carcinomas, colorectal and pancreatic carcinomas, and ovarian cancer (2). Evidence from recent epidemiological studies is also consistent with a role of IGF in tumor development showing a correlation between circulating levels of IGF-I and the relative risk of developing cancer, although some reports show otherwise (3–7).

The IGF system plays a role in cell proliferation and neoplastic growth of the adrenal gland. It has been demonstrated that adrenocortical malignancies overexpress IGF-IR, whereas adenomas or cortical hyperplasia have expression levels similar to the normal tissue (8, 9).

Pheochromocytomas are chromaffin cell-derived neuroendocrine tumors arising from the adrenal medulla, which synthesize, store, and usually secrete catecholamines. Between 13 and 36% of sporadic pheocro-

ISSN Print 0013-7227 ISSN Online 1945-7170
Printed in U.S.A.

doi: 10.1210/en.2012-1107 Received January 26, 2012. Accepted May 7, 2012.

* H.E.C. and M.B. contributed equally to this work.

Abbreviations: Akt, Serine-threonine kinase; BrdU, bromodeoxyuridine; CM, complete medium; FBS, fetal bovine serum; GHR, GH receptor; H&E, hematoxylin and eosin; HS, horse serum; IGF-IR, IGF-I receptor; IR, insulin receptor; LID, liver-IGF-I deficient; LSM, low serum medium; MPC, murine pheochromocytoma; NE, norepinephrine; rh, recombinant human; TUNEL, terminal deoxynucleotidyl transferase 2′-deoxyuridine, 5′-triphosphate nick end labeling; VEGF, vascular endothelial growth factor.

mocytomas undergo malignant transformation, with an overall 5-yr survival of about 50%, but some patients have survived for 20 yr or longer (10, 11). Benign pheochromocytomas have IGF-IR expression levels above those of normal adult adrenomedullary tissue (12), which suggests a possible regulatory role of the IGF-I/IGF-IR circuit in the pathogenesis of the disease.

There are only two pheochromocytoma-derived cell lines available for experimental research, neither of them from humans. One is the PC12 cell line, derived from spontaneous rat pheochromocytomas (13), and the other one is the murine pheochromocytoma (MPC) cell line more recently described. MPC cells are derived from tumors developed in heterozygous neurofibromin (*nf1*) gene knockout mice (14, 15). This cell line expresses the enzyme phenylethanolamine N-methyl transferase required for the synthesis of adrenaline. It also expresses high levels of rearranged during transfection protein, a tyrosine kinase receptor, which is involved in the development of the type 2 multiple endocrine neoplasia syndrome in humans. Therefore, this cell line resembles human pheocromocytoma and is a potential tool for the development of experimental models of the disease (16, 17).

This study was designed to explore the role of IGF-I in the development of pheochromocytoma *in vitro* and *in vivo*. To this end, we used the MPC line and the liver-IGF-I-deficient (LID) mouse model that has a 75% reduction in circulating IGF-I levels (18). We found that IGF-I promotes murine pheochromocytoma development by stimulating proliferation, motility, ability to grow unattached, vessel formation, and by inhibiting apoptosis of pheochromocytoma cells.

Materials and Methods

Pheochromocytoma cell lines

Mouse pheochromocytoma cells (MPC4/30PRR) were kindly provided by A. Tischler (Tufts University, Boston, MA). PC12 cells were purchased from American Type Culture Collection (Manassas, VA).

IGF-I stimulation

PC12 (used as positive control for IGF-IR expression and activation) and MPC cells were cultured and maintained as previously described (14, 19). Cells from both lines were plated on six-well plates, allowed to grow up to 70% confluence, and starved overnight with serum-free medium. Next morning, serum-free medium was refreshed twice (for 2 h and for 15 min) before stimulation with IGF-I. After 5 and 15 min of stimulation with 20 nM recombinant human (rh)IGF-I, cells were harvested on lysis buffer, and proteins were extracted as previously described (20). Experiments were performed in triplicates.

Animal husbandry and PCR genotyping

Mice were housed in standard conditions of 12-h light, 12-h dark cycle with water and food *ad libitum* at the Central Facility, School of Sciences, University of Buenos Aires. The generation of LID mice has been described previously (18). Control mice used in these studies do not express the Cre transgene. Animals (LID and control) backcrossed into the C57BL/6 background were kindly donated by S. Yakar. Mice were genotyped using PCR on tail DNA as previously described (18). All animals were treated and cared in accordance with standard international animal care protocols. All procedures were approved by the Animal Care and Use Committee of the School of Sciences, University of Buenos Aires.

Mouse model of pheochromocytoma

1×10^6 MPC cells were injected sc on the right flank of 8-wk-old male LID (n = 40) and control mice (n = 42). The incidence and latency period of tumor development were recorded up to 12 wk after inoculation. The two longest perpendicular axes in the x/y plane of each developed tumor were measured using vernier caliper for tumor volume calculation (21). Mice were killed when one tumor dimension reached 2 cm.

IGF-I injections

Starting on the day of MPC inoculation, a subgroup of LID mice (n = 18 out of 40) was injected ip twice daily with 2 mg/kg of rhIGF-I (LID+ mice) or with the same volume of saline in control mice (n = 15 out of 42) as described previously (22), until tumors were palpable in the control group. At this time, treatment of LID+ or control mice was withdrawn.

Western blotting

Cell lysates from MPC and PC12 cells were prepared in lysis buffer containing protease inhibitors (23). Briefly, lysates were centrifuged at 12,000 × *g* for 20 min at 4 C; protein concentration in the supernatants was determined using Bradford reagent. Proteins were resolved by SDS-PAGE and transferred to polyvinylidene fluoride membranes. Blots were blocked and probed with various antibodies [antitotal-Erk1/2 (C16), anti-IGF-IR β-subunit (C20), antiinsulin receptor (IR) β-subunit, monoclonal anti-β-actin (clone AC), rabbit polyclonal antiphospho-serine-threonine kinase (Akt) (Ser473), antitotal-Akt, and antiphospho-Erk1/2 (Thr202/Tyr204)]. Western blotting was performed on whole-cell lysates, using 50 μg of protein.

Immunoprecipitation

Lysates from MPC and PC12 cells were spun at 120,000 × *g* for 30 min, and supernatants containing 400 μg of total protein were incubated overnight with 4 μg of anti-IGF-IR antibody. The immunocomplexes were precipitated as described elsewhere (20). Proteins were resolved by SDS-PAGE and were transferred to polyvinylidene fluoride membranes. Blots were blocked and probed with antibodies against tyrosine-phosphorylated proteins (PY20 antibody) and the IGF-IR β-subunit.

Proliferation assay

MPC cells (4×10^5) were seeded on 24-well plates in complete medium (CM) [RPMI 1640, 10% horse serum (HS), 5% fetal bovine serum (FBS)] or in low serum medium (LSM) (8 ×

10^5 cells) (1% HS; 0.5% FBS) and allowed to attach overnight. One plate was used for each point (day) of the assay, and each condition (with or without rhIGF-I) in triplicate, plus an additional plate that was used to determine the initial number of cells (time zero plate). Twenty-four hours after seeding, cells attached to the time zero plate were harvested by trypsinization and counted after 0.5% trypan blue staining. In the remaining plates, medium was replaced by the one containing rhIGF-I to a final concentration of 100 nM for CM or 50 nM for LSM and refreshed every 48 h throughout the experiment. Cells were cultured over 5–7 d, trypsinized, and counted every 48 h.

Bromodeoxyuridine (BrdU) incorporation

MPC cells were seeded in 24-well plates, and on d 5 of culture, cells were incubated with 400 μl of fresh RPMI 1640 media containing 1 mg/ml of BrdU for 1 h at 37 C with 5% CO_2. Cells were then washed with PBS and fixed with methanol:acetic (3:1) for 30 min for immunocitochemitry. DNA denaturation was assessed by incubating the fixed cells with 70% ethanol and 0.2 M NaOH for 3 min followed by cold 70% and then 96% ethanol (1 min each), allowing the plate to dry. To hydrate the cells, three rinses with PBS were performed for 3 min. Endogenous peroxidase and nonspecific sites were blocked with H_2O_2 in 3% methanol and HS in PBS for 30 min, respectively. Finally, cells were incubated with monoclonal BrdU antibody in wet chamber at 4 C overnight. Immunoperoxidase staining was performed according to the manufacturer's recommended protocol for universal labeled streptavidin biotin/system horseradish peroxidase. Nuclei were counterstained with hematoxylin, and over 3000 cells were counted. For *in vivo* BrdU incorporation, mice received an ip injection of BrdU (100 mg/kg body weight) 3 h before killing, and tumors were fixed with 4% paraformaldehyde and embedded in paraffin blocks for immunohistochemistry. BrdU was detected as previously described (24), and a section of intestine from each BrdU-injected mouse was used as positive control.

Apoptosis assays

MPC cells were seeded in 24-well plates and on d 5 of culture were trypsinized, spun, washed with PBS, fixed, placed on eight-well slides, and dried at room temperature. We used a primary rabbit antibody specific for the active, p17 fragment of caspase-3 and a goat antirabbit secondary antibody conjugated to Alexa Fluor 594 fluorochrome (red fluorescence). For DNA fragmentation, we subsequently processed the same slide by the terminal deoxynucleotidyl transferase 2′-deoxyuridine, 5′-triphosphate nick end labeling (TUNEL) method using *In Situ* Cell Death Detection kit as described elsewhere (25, 26). Positive red-stained cells for caspase-3 and green positive nuclei for TUNEL assay were counted under the fluorescence microscope and referred as percentage of total cells observed on the same field, counted on phase. Results were the average of at least 25 fields or 2000 cells.

Soft agar assay

Anchorage-independent growth was assayed by scoring the number and the diameter of colonies formed in 0.4% agarose. Cells were suspended in 3 ml of RPMI 1640 containing 1% HS and 0.5% FBS with or without 50 nM rhIGF-I and plated at a density of 1×10^5 cells per well in 60-mm tissue culture dishes over a bottom layer of 0.5% agarose. Colonies were allowed to develop for 3 wk and counted under a Nikon Eclipse microscope (Nikon, Melville, NY). Each group of cells with a diameter greater than 100 μm (as assessed with a micrometric scale) was considered as a colony.

Cell migration assay

MPC cells were seeded on six-well transwell chambers with 8.0-μm pore size polycarbonate membrane pretreated with collagen. Cells (1×10^5) were added to the upper well, which was placed into a lower well containing RPMI 1640 1% HS, 0.5% FBS, and 50 nM rhIGF-I as a chemoattractant. After 18–24 h of incubation at 37 C in 5% CO_2, the cells remaining on the upper membrane surface were removed with a cotton swab. Cells on the lower surface of the filter were fixed and stained with toluidine blue. Fifteen fields of adherent cells were randomly counted in each well with a Nikon microscope at ×20 magnification, and the results were numerically averaged (20).

Catecholamine measurements

Cell culture

MPC cells were seeded in a six-well plate with serum-free RPMI 1640 media in the presence of 50 nM rhIGF-I. After 6 h of treatment, 1 ml of conditioned media was collected on 200 μl of 0.3 N perchloric acid, and cells were lysed in 500 μl of 0.3 N perchloric acid. Cetecholamines were determined in conditioned media and cell lysates.

Urine samples

Mice were kept in metabolic cages for 12 h before killing for urine collection on 6 N HCl. Catecholamines were partially purified from biological samples by batch alumina extraction, separated by reversed phase HPLC (HPLC-electrochemical detection), and quantified amperometrically (27). Recovery through the alumina extraction step averaged 45–55%.

Pheochromocytoma cell isolation

Tumor tissue was dissected from control, LID, and LID+IGF-I mice and cut into small fragments to be digested with trypsin-EDTA at 37 C for 7 min with constant stirring (28). Three volumes of fresh RPMI 1640 CM were added, and the supernatant was collected by aspiration, transferred to a sterile tube, and cells were collected by centrifugation at $200 \times g$ for 10 min. Cells were resuspended in 2 ml of fresh RPMI 1640 CM, seeded on top of a 60% Percoll solution, and centrifuged at $800 \times g$ for 30 min. This procedure resulted in the removal of red blood cells. Cells obtained in the 0–60% interface were collected, washed with PBS, and centrifuged at $600 \times g$ for 5 min. Tumor cells were lysed for Western blot analysis as described above.

Histology and immunohistochemistry

Tumors were removed and fixed in 4% paraformaldehyde. Tissues were then embedded in paraffin, and consecutive 5-μm sections were cut and mounted on glass slides. Sections were stained with hematoxylin and eosin (H&E) and Masson's trichromic staining according to standard protocols. Anti-IGF-IR rabbit polyclonal antibody (1:200 dilution) and antifactor VIII rabbit polyclonal antibody (1:250 dilution) were used as

primary antibodies. Immunoperoxidase staining was performed according to the manufacturer's recommended protocol for Avidin- Biotin complex and 3,3′-diaminobenzidine substrate kits. For positive controls, human breast cancer sections were stained for IGF-IR as well as for factor VIII. For negative controls, all reagents except primary antibodies were used. Vessel counting was assessed as the number of positive cells for factor VIII (29). Cleaved caspase-3 and TUNEL were performed following standard protocols for inmunofluorescence tissue labeling with the antibodies and materials described above (apoptosis assays).

Chemicals and antibodies

Chemicals, culture materials, and antibodies were obtained from the following sources: six- and 24-well plates (Corning, Lowell, MA), RPMI 1640, HS, and FBS (GIBCO, Grand Island, NY), trypsin-EDTA (Invitrogen, Carlsbad, CA), rhIGF-I (Genentech, Inc., San Francisco, CA), six-well transwell chambers (BD Biosciences, San Diego, CA), eight-well slides (CellPoint, Gaithersburg, MD), BrdU and Percoll (Sigma, St. Louis, MO), protease inhibitors (Complete Mini EDTA free) and *In Situ* Cell Death Detection kit (peroxidase) (Roche Diagnostics, Indianapolis, IN), Bradford reagent (Bio-Rad Laboratories, Philadelphia, PA), labeled streptavidin biotin/system horseradish peroxidase and Chromogen System (Dako, Carpinteria, CA), and ABC kit and DAB substrate kit (Vector Laboratories, Burlingame, CA). For antibodies, rabbit polyclonal antibodies to total-Erk1/2 (C16) and IGF-IR β-subunit (C20) were purchased from Santa Cruz Biotechnology, Inc. (Santa Cruz, CA). Monoclonal anti-β-actin (clone AC) was obtained from Sigma. Rabbit polyclonal antibodies to phospho-Akt (Ser473), total-Akt, and phospho-Erk1/2 (Thr202/Tyr204) were from New England Biolabs (Beverly, MA); tyrosine-phosphorylated proteins (PY20 antibody) were from Transduction Laboratories (Lexington, KY); p17 subunit of caspase-3 from Cell Signaling Technology (Danvers, MA); and antifactor VIII rabbit polyclonal antibody from Dako.

Statistical analysis

Two-tailed Mann-Whitney *U* nonparametric test or Student's *t* test was used for analyzing differences between basal and IGF-I-treated conditions for *in vitro* studies. Log-rank test was used to analyze the differences in incidence and latency period between control, LID, and LID+IGF-I mice from survival curves. One-way ANOVA was used for comparisons between more than two groups of data. Unless specified, all values are reported as mean ± SE, and statistical significance was accepted at $P < 0.05$.

Results

MPC cells express a functional IGF-IR

In culture, MPC cells grow in epithelial-like clusters attached to the culture plate, with spontaneous extension of neurites. They have scarce cytoplasm and are positive for IGF-IR immunolabeling (Fig. 1, A and B). To assess IGF-IR activation, we performed immunoprecipitation of the IGF-IR after rhIGF-I stimulation and blotted the membranes for tyrosine phosphorylated proteins and analyzed, by direct application, the phosphorylation status of two major components of the signaling cascade of the IGF-IR. PC12 cell lysates were used as positive control. As shown in Fig. 1C, upon 5–15 min with 20 nM IGF-I stimulation, MPC and PC12 cell lysates showed tyrosine phosphorylation of the IGF-IR as well as phosphorylation of AKT and ERK 1/2. These results indicate that MPC cells express an intact IGF-IR that is activated upon IGF-I stimulation *in vitro*. Therefore, we continued our experiments using only MPC cells.

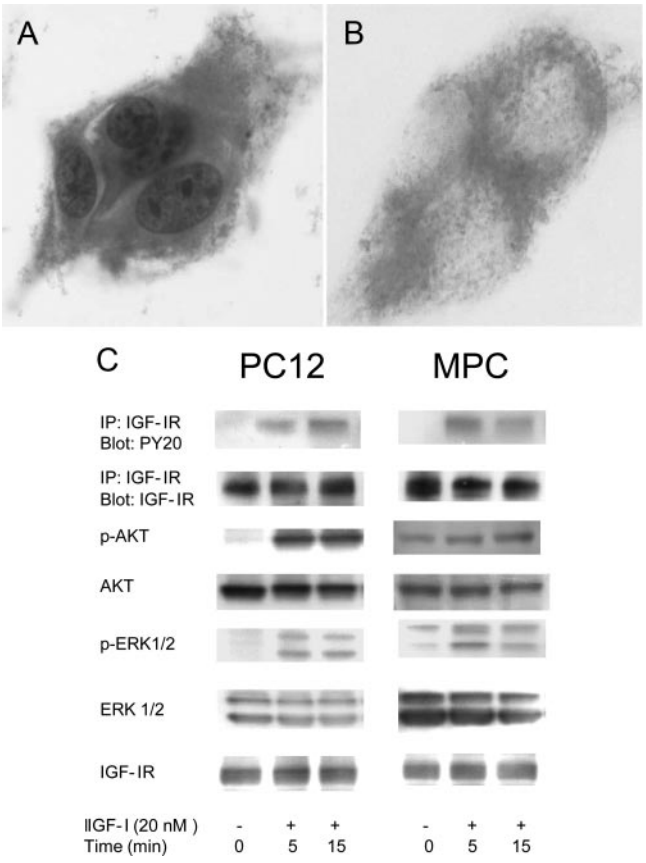

FIG. 1. Expression and activation of IGF-IR in MPC cells. A, Representative microphotography of MPC cells organized in epithelial-like clusters stained with H&E. B, Immunocytochemistry revealing the expression of the IGF-IR. C, Western blotting of MPC cell lysates immunoprecipitation (IP) of the IGF-IR and direct application after rhIGF-I stimulation for 0, 5, or 15 min. Membranes were blotted with antiphosphotyrosine (PY20) or anti-IGF-IR (lines 1 and 2), antiphospho-AKT (p-AKT), antiphospho-ERK (p-ERK1/2), or anti-IGF-IR (lines 3, 5, and 7). Blots were stripped and reprobed with antitotal-AKT (AKT) or antitotal-ERK (ERK1/2) in lines 4 and 6.

IGF-I stimulates proliferation and inhibits apoptosis in MPC cells but does not change cell catecholamine content or secretion

The effects of IGF-I on cell proliferation and inhibition of apoptosis have been described in several types of normal and tumor cells (2). To asses these effects on MPC cells, we performed proliferation assays with and without IGF-I stimulation in two different culture conditions, one in CM

and the other one with serum deprivation (LSM). A significant increase in cell number was noted on cells in CM cultures upon rhIGF-I stimulation (Fig. 2A, *left panel*). Spontaneous MPC cell proliferation was blunted on LSM, but addition of rhIGF-I resulted in a significant stimulation (Fig. 2A, *right panel*).

To further characterize the observed effect of IGF-I on MPC cell cultures, we performed BrdU incorporation, cleaved caspase-3 detection, and TUNEL assay on d 5 of culture. As shown in Fig. 2B, rhIGF-I stimulation increased BrdU incorporation from 37 ± 8 to 50 ± 5% in CM (Fig. 2B, *left panel*) and from 26 ± 6 to 35 ± 6% in LSM (Fig. 2B, *right panel*). BrdU incorporation on LSM condition in the absence of IGF-I was higher than expected, considering that the number of cells did not increase under this culture condition (Fig. 2A, *right panel*). Therefore, we decided to analyze whether these cells were undergoing apoptosis. Apoptotic cells were detected by immunofluorescence for cleaved caspase-3 and TUNEL assay for DNA fragmentation. There were no differences in the apoptotic index observed in basal compared with rhIGF-I-stimulated condition with CM (Fig. 2C, *left panel*). Conversely, in LSM the percentage of apoptotic cells (assessed by either cleaved caspase-3 or TUNEL staining) was significantly reduced in cells treated with rhIGF-I (Fig. 2C, *right panel*).

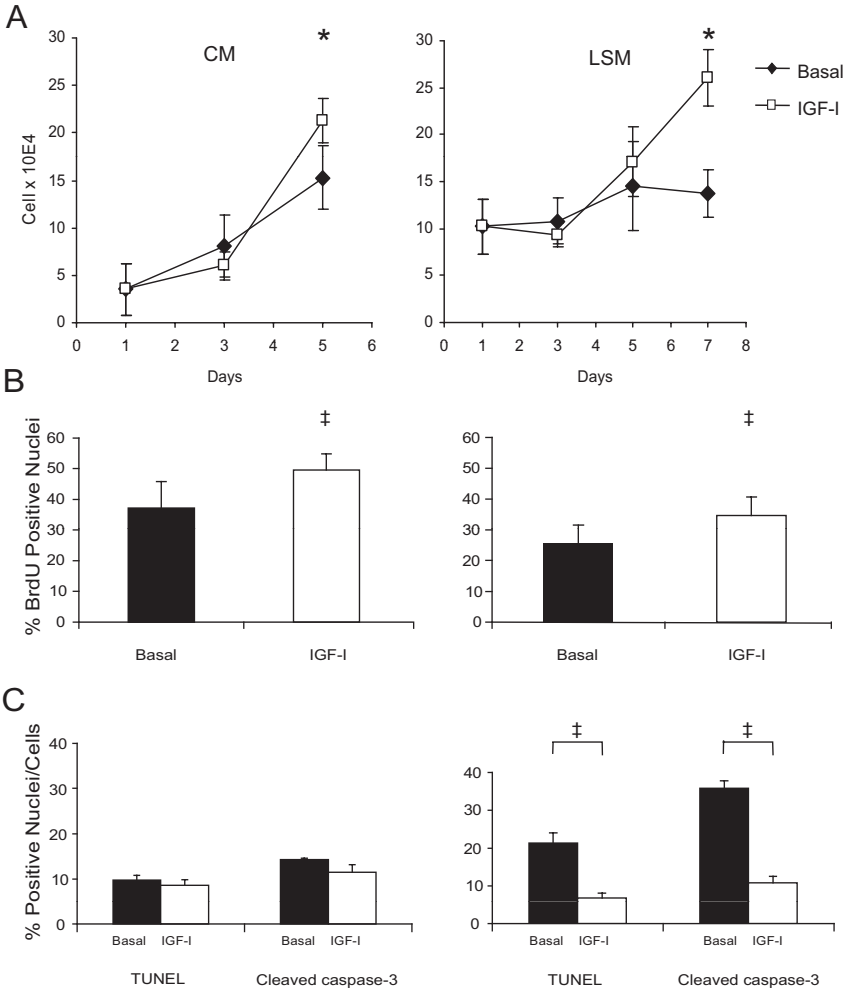

FIG. 2. Proliferative and antiapoptotic effects of IGF-I on MPC cells. A, MPC cells were grown in CM (3×10^4 cells/well) or LSM (8×10^4 cells/well) with (*open squares*) or without (*closed diamonds*) rhIGF-I. Results of a representative experiment from a total of five performed in triplicates are shown. B, On d 5, MPC cells grown on CM (*left panel*) or LSM (*right panel*) in the absence (*closed bars*) or presence (*open bars*) of rhIGF-I and were incubated with BrdU for 1 h. Positive nuclei were quantified. Results are expressed as mean ± SE from three independent experiments. C, Apoptosis assays. MPC cells were collected on d 5 to asses DNA fragmentation by TUNEL assay and the activation of caspase-3 in CM or LSM in the absence (closed bars) or presence (*open bars*) of rhIGF-I. Green positive nuclei for TUNEL assay and positive red-stained cells for caspase-3 were counted in 25 random fields, and results are expressed as mean ± SE from three independent experiments. *, $P < 0.05$, unpaired *t* test; ‡, $P < 0.01$, Mann-Whitney *U* test.

Bach and Leeding (30) have shown that IGF-I modulates catecholamine content in PC12 cells. In our hands, norepinephrine (NE) content and secretion by MPC cells to conditioned media was not modified after 6 h rhIGF-I stimulation (in nanograms of NE/1000 cells, mean ± SE; cell lysates basal, 6.96 ± 0.80 and IGF-I, 6.77 ± 1.27; conditioned media basal, 9.44 ± 4.42 and IGF-I, 6.78 ± 1.65; *P* value not statistically significant, Mann-Whitney *U* test).

IGF-I exacerbates tumorigenic characteristics of MPC cells

We examined migration and anchorage-independent growth in soft agar, two major characteristics of tumor cells that best correlate with *in vivo* tumorigenicity (30, 31). To assess these properties, MPC cells were plated in soft agar and incubated with or without rhIGF-I for 21 d. Representative photos are shown in Fig. 3, A and B. Spontaneous colony formation was significantly stimulated by rhIGF-I, which increased the number and size of colonies formed during the assay (Fig. 3, A and B, *right panels*).

To study the effect of IGF-I on migration, MPC cells where seeded in transwell chambers with or without rhIGF-I for 24 h. The number of MPC cells that migrated to the bottom chamber significantly increased under rhIGF-I stimulation (Fig. 3C)

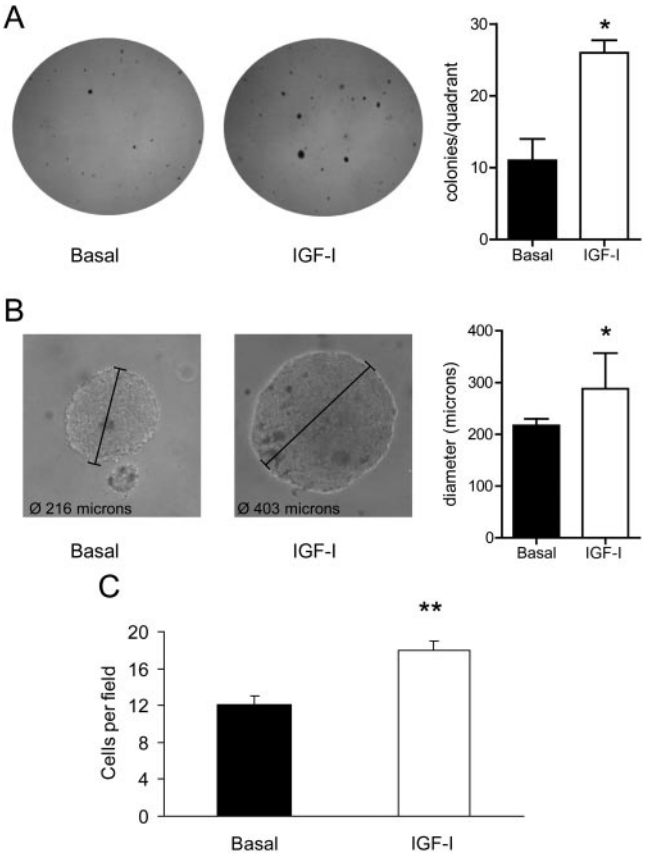

FIG. 3. IGF-I enhances MPC colony formation and migration. MPC cells were plated over a bottom layer of 0.5% agarose with or without IGF-I stimulation, and colonies were allowed to develop for 3 wk. A, *Left and middle panels*, Representative fields of colony formation assays. Quantification is shown on the *right*. B, Representative colonies under basal (*left panel*) and IGF-I-stimulated (*middle panel*) conditions. The *right panel* shows the colony size (diameter) quantification. C, MPC cells (1×10^5 cells) were seeded on six-well transwell chambers with (*open bars*) or without (*closed bars*) rhIGF-I. After 18–24 h of incubation, migrated cells were fixed and stained with toluidine blue. Fifteen fields of adherent cells were randomly counted. Results are expressed as mean ± SE from three independent experiments. *, $P <$ 0.05, unpaired *t* test; **, $P < 0.01$, Mann-Whitney *U* test.

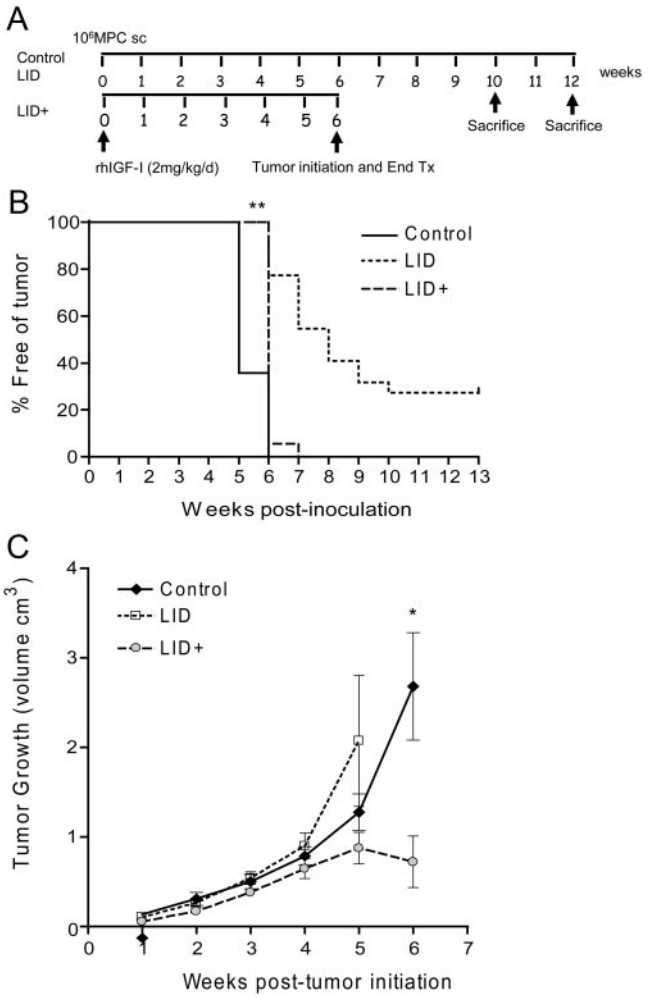

FIG. 4. Effect of reduced circulating IGF-I levels on tumor incidence and growth. A, Schematic representation of the experimental design. MPC cells were inoculated sc in control and LID mice. A subset of LID mice was treated with rhIGF-I (2 mg/kg·d) (LID+) until tumors developed in control mice. B, The incidence and latency period of tumor development was recorded and plotted in a Kaplan-Meyer curve (control, n = 42, *solid line*; LID, n = 22, *pointed line*; LID+, n = 18, *dashed line*). C, For each developed tumor, the two longest perpendicular axes in the x/y plane were measured, and the volume was calculated. Results are expressed as mean ± SE (control, *solid line*; LID, *pointed line*; LID+, *dashed line*). **, $P < 0.001$, Log-rank test, LID *vs.* control and LID *vs.* LID+; *, $P < 0.01$, Mann-Whitney *U* test, control *vs.* LID+.

IGF-I deficiency decreases tumor incidence and prolongs the latency period of MPC

Results obtained *in vitro* do not always reflect the situation *in vivo*. Therefore, to address whether the *in vitro* effects of IGF-I on MPC cells were functionally relevant *in vivo*, we next generated a model for pheochromocytoma development. We inoculated MPC cells sc in C57B6 background male mice and compared tumor development and characteristics with those developed in LID mice of the same genetic background. A subset of LID mice (n = 18) was treated with rhIGF-I (LID+) from the time of cell inoculation until the time of tumor initiation (palpable tumors) in the corresponding control group (6 wk) when the treatment was ended (Fig. 4A). A total of 82 mice were analyzed for tumor growth. As shown in Fig. 4B, 100% (n = 42) of control mice developed palpable tumors 5–6 wk after cell inoculation. In contrast, in 16 out of 22 LID mice (73%), tumor development was delayed to 7–12 wk after cell inoculation, and the remaining six (27%) did not develop tumors up to 12 wk after inoculation (Log-rank test, $P < 0.001$; control *vs.* LID). Similarly to controls, all LID+ mice developed tumors between 5 and 6 wk after cell inoculation (Log-rank test, $P < 0.001$; LID+ *vs.* LID) (Fig. 4B). In addition, the latency period until appearance of a palpable mass in 50% of mice was 2 wk shorter in control and LID+ mice than that observed in LID mice (6 *vs.* 8 wk).

Tumor growth was similar in LID compared with control mice (Fig. 4C). Tumor growth in LID+ mice was similar to LID and control groups only until wk 4 from tumor initiation (wk 10 after cell inoculation). At this point, the growth rate decreased, and tumors from LID+ mice became smaller and remained smaller until the end of the experiment. Moreover, three out of the 18 LID+ mice had complete tumor regression.

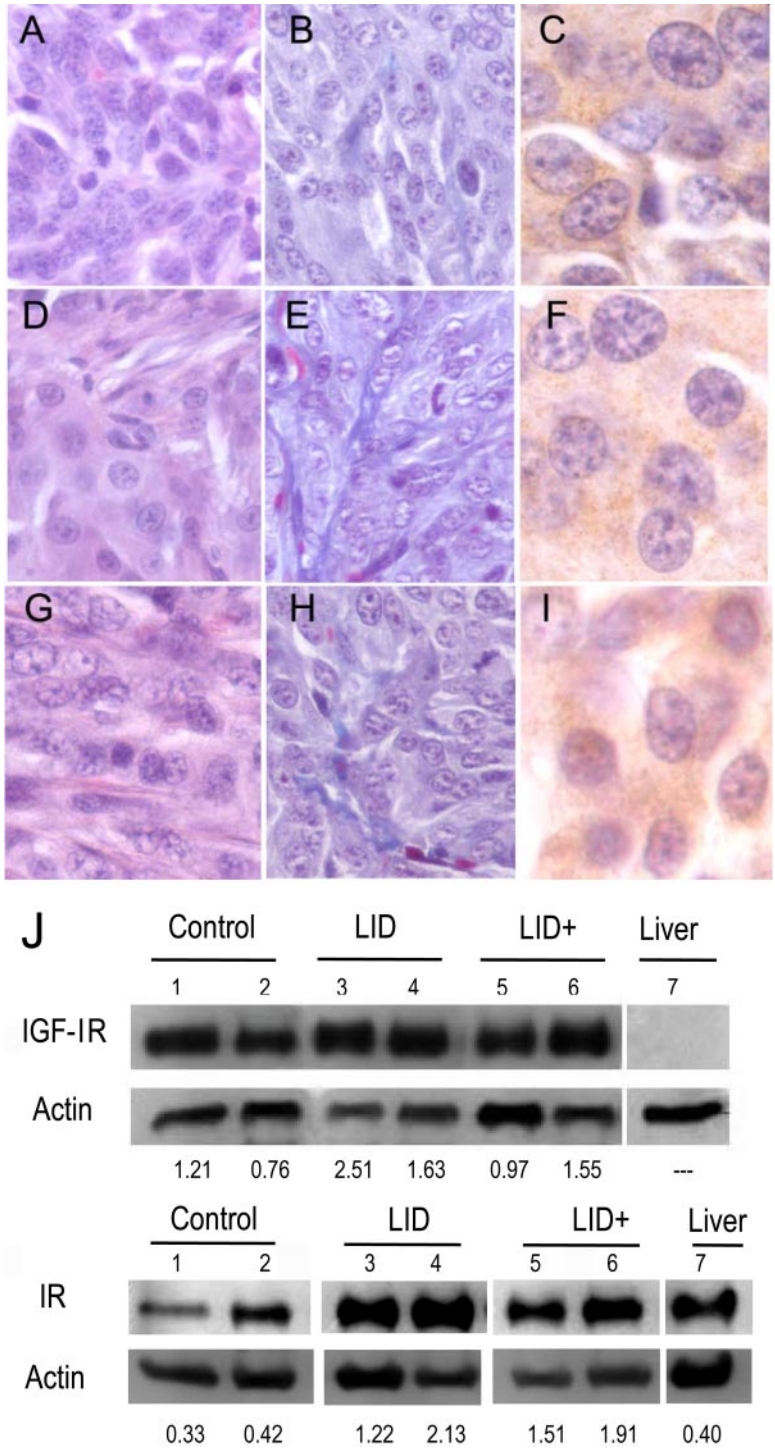

FIG. 5. Representative fields of tumor histology are depicted for control (A–C), LID (D–F), and LID+ (G–I) mice. H&E staining (A, D, and G), Masson´s trichrome staining (B, E, and H), and immunohistochemistry of IGF-IR expression (C, F, and I). J, Representative Western blotting for IGF-IR and IR expression. Protein extracts of isolated cells from tumors developed in control, LID, and LID+ mice were probed for IGF-IR, IR, and β-actin. *Numbers below the picture* represent the ratio IGF-IR/β-actin and IR/β-actin.

Histology and functional characteristics

Tumors developed in control, LID, and LID+ mice had similar histologic characteristics. They were highly cellular with little stromal tissue (Fig. 5, A, D, and G). Tumor cells had scant cytoplasm, round to oval euchromatic nuclei, and gathered in well formed nests separated by thin connective tissue septa with capillaries (Fig 5, B, E, and H). This histology was very reminiscent to that of pheochromocytomas. IGF-IR expression was similarly positive in tumors from the three experimental groups (Fig. 5, C, F, and I). These immunohistochemical observations were confirmed by investigating IGF-IR expression by immunoblot in total lysates of isolated tumor cells from control, LID, and LID+ mice. As shown in Fig. 5J, *upper panels*, tumor IGF-IR expression was similar among all groups. The expression of IR was also investigated by immunoblot (Fig. 5J, *lower panels*). Densitometric analysis of the ratio IR/actin shows that the IR expression is significantly higher in tumors form LID and has a tendency to be higher in tumors from LID+ mice compared with those from control mice (0.34 ± 0.06 *vs.* 1.8 ± 0.42 C *vs.* LID, $P < 0.05$; 0.034 ± 0.06 *vs.* 1.91 ± 0.83 $P = 0.06$, not statistically significant, Mann-Whitney *U* test)

Catecholamine synthesis and secretion are identifying features of pheochromocytomas. We measured 12 h of urinary excretion of NE in urine samples collected from control and LID mice 3 wk after tumor development. As expected, NE excretion was significantly increased in tumor-bearing animals compared with their noninoculated corresponding controls (NE μg/12 h, mean $\pm$ SE; control mice, 0.17 ± 0.02 *vs.* 1.40 ± 0.21; LID mice,

0.24 ± 0.05 *vs.* 1.75 ± 0.39 $P < 0.05$ noninoculated *vs.* inoculated, Mann-Whitney test) .

IGF-I deficiency decreases vascular density and increases apoptosis of MPC

Vascular density was assessed by immunostaining for factor VIII as a marker for endothelial cells. As shown in Fig. 6A, tumors from LID and LID+ mice had a significant decrease in vessel density compared with tumors from control mice.

In vivo BrdU incorporation revealed a significant increase of DNA synthesis (cell proliferation) in tumors from LID and LID+ mice compared with those developed in control mice (Fig. 6B). TUNEL assay and cleaved caspase-3 labeling showed that the percentage of apoptotic cells found in tumors from LID mice was higher than that found in tumors from control mice but lower than the one observed in tumors from LID+ mice (Fig. 6C). These observations could explain, at least in part, the stabilization or decline in tumor volume observed in LID+ mice (Fig. 4C) 5–6 wk after the end of the treatment with rhIGF-I.

Discussion

Our results demonstrate that IGF-I promotes murine pheochromocytoma development, at least in part, by promoting cell proliferation, migration, ability to grow unattached, and inhibition of apoptosis of MPC cells. *In vivo*, IGF-I deficiency decreases vascular density, tumor incidence, and prolongs the latency period for tumor growth of MPC. Treatment with rhIGF-I during the latency period (LID+) restores tumor incidence to control values and shortens the latency period for tumor development.

Previous studies have shown the presence of IGF-IR in PC12 cells, a cell line derived from spontaneous pheochromocytomas occurring in rats. In this model, IGF-I stimulation increased cellular proliferation and survival (32, 33). It has also been shown that IGF-I stimulates proliferation and survival of rat chromaffin cells of the adrenal medulla during neonatal growth and in the adult (34). However, information regarding the effects of IGF-I on pheochromocytoma cells is still scarce. The present study shows by the first time that IGF-I stimulation promotes tumor growth, inhibits apoptosis, and enhances aggressive phenotype of MPC cells.

Avoidance from apoptosis and a perpetual replicative potential are two hallmarks of cancer (35). Cumulative evidence has been obtained concerning the role of the IGF/IGF-IR circuit in the emergence and progression of cancer.

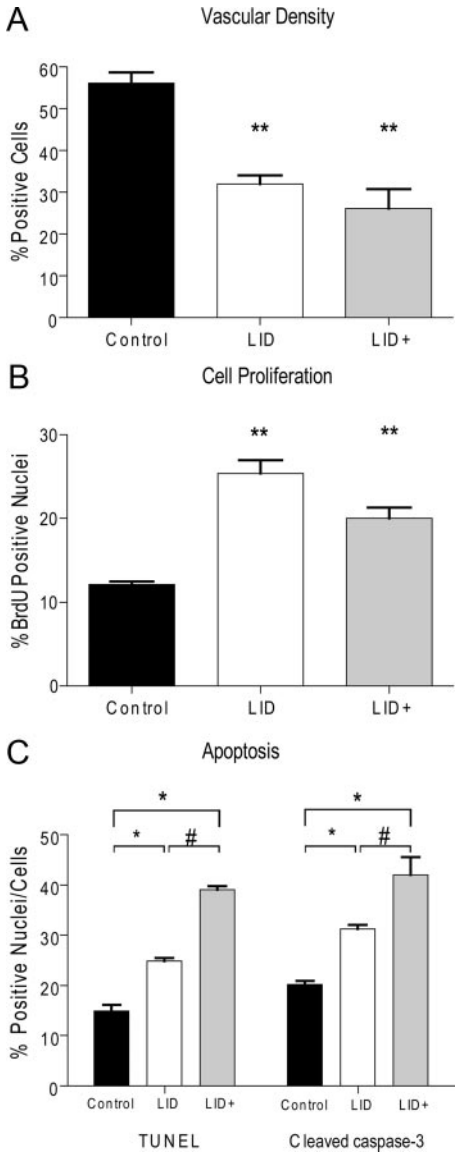

FIG. 6. Vascular density, proliferation, and apoptotic index in pheochromocytomas with 4 wk of evolution from control (*closed bars*), LID (*open bars*), and LID+ (*gray bars*) mice. A, Vascular density was assessed by immunostaining for factor VIII as a marker for endothelial cells. Results are expressed as mean ± SE. B, Proliferation index *in vivo*. Mice were injected with BrdU 3 h before killing. Tumor positive nuclei were quantified. Results are expressed as mean ± SEM from three independent experiments. C, Apoptotic index. Tumors embedded in paraffin blocks were sliced to perfom TUNEL and cleaved caspase-3 assays. Green positive nuclei for TUNEL assay and red-stained cells for caspase-3 were counted and referred as percentage of total cells observed on the same field. Results are expressed as mean ± SE; **, $P < 0.001$ LID and LID+ *vs.* control; *, $P < 0.01$ LID and LID+ *vs.* control.; #, $P < 0.01$ LID *vs.* LID+, ANOVA Kruskal-Wallis, Dunns test.

IGF-IR was found to be essential for oncogenic transformation in certain cellular systems. Mouse fibroblasts lacking IGF-IR cannot be transformed by known oncogenes, such as simian virus 40 T antigen, papillomavirus E5, and overexpression of Ras (36). On the other hand, overexpression of a constitutively activated IGF-IR was shown to

be sufficient to cause mammary epithelial cell transformation in mouse models (37, 38). In prostate epithelial cells, however, reexpression of the IGF-IR inhibited the malignant phenotype of simian virus 40 T antigen immortalized human prostate epithelial cells (39). Also, epithelial-specific deletion of IGF-IR accelerated the emergence of aggressive prostate cancer when p53 activity was compromised (40). These observations underscore the importance of the IGF axis in carcinogenesis and tumor progression but also demonstrate that IGF-I effects are variable in different cell and tissue types, including cancer. The present results demonstrate that IGF-I has a critical role on the survival and malignant behavior of MPC cells. When injected sc, MPC cells survived and formed tumors in 100% of mice that had normal levels of circulating IGF-I. On the contrary, when circulating levels of IGF-I were low, tumor development was delayed or even prevented.

Epidemiological studies have revealed that high IGF-I serum concentrations are associated with breast, colorectal, and prostate cancer (5), and more recently, an IGF-I polymorphism has been associated with nonsmall cell lung cancer (41). LID mice have been well characterized and are a suitable model to study tumor development in the context of IGF-I deficiency (22, 42–44). Our results using this model support the idea that IGF-I is critical for the survival of these cells *in vivo*, at the point of injection. Furthermore, LID mice have increased levels of GH, as a result of decreased IGF-I levels, and elevated basal insulin levels (18, 45, 46). The effects of GH and insulin on tumor growth and development and the presence of GH receptor (GHR) and IR in normal and tumoral adrenal medulla have also been described (47, 48). We have confirmed the expression of IR in cell lysates from tumors harbored by LID and control mice. However present, elevated GH and insulin levels are not enough to compensate for the decreased IGF-I effect and therefore to promote pheochromocytoma development in all IGF-I deficient mice. The crucial role of IGF-I in tumor establishment was confirmed by the fact that when LID mice were treated with rhIGF-I from the time of cell inoculation until wk 6 (when the treatment was withdrawn), tumor incidence equaled that of control mice, underscoring the importance of IGF-I during the initial establishment of these tumors.

Once established, tumors from LID and control mice grew at a similar rate, which could be explained if cells that survived on a context of decreased IGF-I (LID mice) had either become IGF-I independent or acquired an increased sensitivity to IGF-I. Although the expression of IGF-IR in tumor cells from both LID and control mice showed no differences between groups, the expression of the IR was higher in tumor cells from LID compared with control mice, supporting a possible role of insulin in tumor growth in LID mice. Regarding the GHR, we did not have the possibility to test whether this receptor expression was increased or changed in our samples. However, there is at least one recent report (42), where in a mouse model of prostate tumors developed in LID mice, a low systemic IGF-I environment coupled with higher GH levels was associated with compensatory increases in the expression of the GHR in prostate tumor cells. We speculate that in our model, with a similar context of tumor development, it is possible that similar changes in the expression of the GHR are taking place in pheochromocytoma cells. Thus, it is also possible that the proliferation of the established tumors in an environment of low IGF-I is dependent on growth factors other than IGF-I, such as insulin or GH.

The effects of IGF-I on inhibition of apoptosis have been vastly documented (2). In our model, the *in vitro* effect of IGF-I on MPC cells apoptosis was also observed *in vivo*, where the IGF-I deficiency had a potent effect on intratumor apoptosis. This was higher in tumors from LID mice compared with those from control mice, which could explain why, despite having higher proliferation rate, tumors from LID and control mice have similar volume.

Angiogenic potential is important for tumor growth and dissemination. Several growth factors, such as angiogenin and vascular endothelial growth factor (VEGF), have a critical role in angiogenesis. Correlations between VEGF expression and vascular density have been documented in primary breast cancer specimens and gastric carcinomas (49, 50). Also, it has been shown that IGF-I stimulates VEGF production in different types of cells (22, 51). We also observed that IGF-I stimulation up-regulates VEGF expression in MPC cells (data not shown). In our model, tumors developed in the context of low circulating IGF-I have a decreased vascular density compared with controls. Again, neither GH nor insulin could compensate for IGF-I deficiency on apoptotic index and vascular density. These results strongly suggest that circulating IGF-I determines angiogenesis and apoptosis in MPC.

For the present study, we chose a rhIGF-I dose that had been previously used in LID mice and other experimental models and treated cell inoculated LID mice (LID+) during the latency period to tumor development. Using this scheme of treatment, serum IGF-I levels in LID mice reached values similar to control mice, and GH and insulin levels were reduced and normalized during the period of IGF-I administration (22, 45). Treatment of LID mice with rhIGF-I for 5–6 wk after cell inoculation restored tumor incidence. However, tumor volume and vascular density remained lower in tumors harbored by LID+ mice. As discussed above, the depletion of systemic IGF-I in LID mice may induce the selection of cells that are less sensitive

to IGF-I, and more dependent for cellular proliferation on GH and insulin that are elevated in this model. However, two major aspects of tumor development, such as vessel formation and avoidance from apoptosis, remained dependent of IGF-I. We propose that in LID+ mice, the initial treatment with rhIGF-I could have prevented the "selection" that occurred in LID-untreated mice, resulting in the establishment of tumors that are more dependent on IGF-I for survival. Once treatment is ended, these tumors are exposed to the low systemic levels of IGF-I. As a consequence, tumors harbored by LID+ mice show a higher apoptotic index and a low vessel density. Taken together, these results provide support to our hypothesis that IGF-I is important for cell survival at the point of injection, vessel formation, and survival of intratumoral cells.

In summary, our work demonstrates that IGF-I has a critical role in maintaining tumor phenotype and survival of already transformed pheochromocytoma cells, and it is required for the initial establishment of these tumors. Our work provides encouragement to carry on research studies to address the IGF-I/IGF-IR circuit as a possible target of therapeutic strategies for pheochromocytoma treatment in the future.

Acknowledgments

We thank Mr. Eduardo Dascal, Licenciado Cristian Alvarez Sedó, and Dr. Fernanda Riera for their expert technical assistance.

Address all correspondence and requests for reprints to: Patricia A. Pennisi, Ph.D., Centro de Investigaciones Endocrinológicas Consejo Nacional de Investigaciones Científicas y Técnicas, Hospital de Niños Dr. Ricardo Gutiérrez, Gallo 1360, C1425EFD Buenos Aires, Argentina. E-mail: ppennisi@cedie.org.ar.

This work was supported by the Ministerio de Ciencia y Tecnología (Mincyt, Agencia de Promoción Científica y Tecnológica) Grant PICT06-01002 (to P.A.P.) and by the Consejo Nacional de Investigaciones Científicas y Tecnológicas (CONICET) Argentina Grant PIP08-1905 (to P.A.P.). M.C.F. is a Ph.D. student and has a doctoral fellowship from CONICET.

Disclosure Summary: The authors have nothing to disclose.

References

1. **Jones JI, Clemmons DR** 1995 Insulin-like growth factors and their binding proteins: biological actions. Endocr Rev 16:3–34
2. **Samani AA, Yakar S, LeRoith D, Brodt P** 2007 The role of the IGF system in cancer growth and metastasis: overview and recent insights. Endocr Rev 28:20–47
3. **Ma J, Pollak MN, Giovannucci E, Chan JM, Tao Y, Hennekens CH, Stampfer MJ** 1999 Prospective study of colorectal cancer risk in men and plasma levels of insulin-like growth factor (IGF)-I and IGF-binding protein-3. J Natl Cancer Inst 91:620–625
4. **Yu H, Spitz MR, Mistry J, Gu J, Hong WK, Wu X** 1999 Plasma levels of insulin-like growth factor-I and lung cancer risk: a case-control analysis. J Natl Cancer Inst 91:151–156
5. **Renehan AG, Zwahlen M, Minder C, O'Dwyer ST, Shalet SM, Egger M** 2004 Insulin-like growth factor (IGF)-I, IGF binding protein-3, and cancer risk: systematic review and meta-regression analysis. Lancet 363:1346–1353
6. **Platz EA, Pollak MN, Leitzmann MF, Stampfer MJ, Willett WC, Giovannucci E** 2005 Plasma insulin-like growth factor-1 and binding protein-3 and subsequent risk of prostate cancer in the PSA era. Cancer Causes Control 16:255–262
7. **Severi G, Morris HA, MacInnis RJ, English DR, Tilley WD, Hopper JL, Boyle P, Giles GG** 2006 Circulating insulin-like growth factor-I and binding protein-3 and risk of prostate cancer. Cancer Epidemiol Biomarkers Prev 15:1137–1141
8. **Boulle N, Logié A, Gicquel C, Perin L, Le Bouc Y** 1998 Increased levels of insulin-like growth factor II (IGF-II) and IGF-binding protein-2 are associated with malignancy in sporadic adrenocortical tumors. J Clin Endocrinol Metab 83:1713–1720
9. **Weber MM, Auernhammer CJ, Kiess W, Engelhardt D** 1997 Insulin-like growth factor receptors in normal and tumorous adult human adrenocortical glands. Eur J Endocrinol 136:296–303
10. **Nomura K, Kimura H, Shimizu S, Kodama H, Okamoto T, Obara T, Takano K** 2009 Survival of patients with metastatic malignant pheochromocytoma and efficacy of combined cyclophosphamide, vincristine, and dacarbazine chemotherapy. J Clin Endocrinol Metab 94:2850–2856
11. **Zarnegar R, Kebebew E, Duh QY, Clark OH** 2006 Malignant pheochromocytoma. Surg Oncol Clin N Am 15:555–571
12. **Fottner C, Minnemann T, Kalmbach S, Weber MM** 2006 Overexpression of the insulin-like growth factor I receptor in human pheochromocytomas. J Mol Endocrinol 36:279–287
13. **Greene LA, Tischler AS** 1976 Establishment of a noradrenergic clonal line of rat adrenal pheochromocytoma cells which respond to nerve growth factor. Proc Natl Acad Sci USA 73:2424–2428
14. **Powers JF, Schelling KH, Brachold JM, Tischler AS** 2002 Plasticity of pheochromocytoma cell lines from neurofibromatosis knockout mice. Ann NY Acad Sci 971:371–378
15. **Powers JF, Schelling K, Brachold JM, Tsokas P, Schayek H, Friedman E, Tischler AS** 2002 High-level expression of receptor tyrosine kinase Ret and responsiveness to Ret-activating ligands in pheochromocytoma cell lines from neurofibromatosis knockout mice. Mol Cell Neurosci 20:382–389
16. **Martiniova L, Ohta S, Guion P, Schimel D, Lai EW, Klaunberg B, Jagoda E, Pacak K** 2006 Anatomical and functional imaging of tumors in animal models: focus on pheochromocytoma. Ann NY Acad Sci 1073:392–404
17. **Ohta S, Lai EW, Taniguchi S, Tischler AS, Alesci S, Pacak K** 2006 Animal models of pheochromocytoma including NIH initial experience. Ann NY Acad Sci 1073:300–305
18. **Yakar S, Liu JL, Stannard B, Butler A, Accili D, Sauer B, LeRoith D** 1999 Normal growth and development in the absence of hepatic insulin-like growth factor I. Proc Natl Acad Sci USA 96:7324–7329
19. **Tischler AS, Greene LA** 1978 Morphologic and cytochemical properties of a clonal line of rat adrenal pheochromocytoma cells which respond to nerve growth factor. Lab Invest 39:77–89
20. **Pennisi PA, Barr V, Nunez NP, Stannard B, Le Roith D** 2002 Reduced expression of insulin-like growth factor I receptors in MCF-7 breast cancer cells leads to a more metastatic phenotype. Cancer Res 62:6529–6537
21. **Jensen MM, Jørgensen JT, Binderup T, Kjaer A** 2008 Tumor volume in subcutaneous mouse xenografts measured by microCT is more accurate and reproducible than determined by 18F-FDG-microPET or external caliper. BMC Med Imaging 8:16
22. **Wu Y, Yakar S, Zhao L, Hennighausen L, LeRoith D** 2002 Circu-

lating insulin-like growth factor-I levels regulate colon cancer growth and metastasis. Cancer Res 62:1030–1035
23. **Dupont J, Karas M, LeRoith D** 2000 The potentiation of estrogen on insulin-like growth factor I action in MCF-7 human breast cancer cells includes cell cycle components. J Biol Chem 275:35893–35901
24. **Pennisi PA, Kopchick JJ, Thorgeirsson S, LeRoith D, Yakar S** 2004 Role of growth hormone (GH) in liver regeneration. Endocrinology 145:4748–4755
25. **Mirkes PE, Little SA, Umpierre CC** 2001 Co-localization of active caspase-3 and DNA fragmentation (TUNEL) in normal and hyperthermia-induced abnormal mouse development. Teratology 63: 134–143
26. **Rawe VY, Boudri HU, Alvarez Sedó C, Carro M, Papier S, Nodar F** 2010 Healthy baby born after reduction of sperm DNA fragmentation using cell sorting before ICSI. Reprod Biomed Online 20: 320–323
27. **Eisenhofer G, Goldstein DS, Stull R, Keiser HR, Sunderland T, Murphy DL, Kopin IJ** 1986 Simultaneous liquid-chromatographic determination of 3,4-dihydroxyphenylglycol, catecholamines, and 3,4-dihydroxyphenylalanine in plasma, and their responses to inhibition of monoamine oxidase. Clin Chem 32:2030–2033
28. **Pellizzari EH, Barontini M, Figuerola Mde L, Cigorraga SB, Levin G** 2008 Possible autocrine enkephalin regulation of catecholamine release in human pheochromocytoma cells. Life Sci 83:413–420
29. **Weidner N, Semple JP, Welch WR, Folkman J** 1991 Tumor angiogenesis and metastasis-correlation in invasive breast carcinoma. N Engl J Med 324:1–8
30. **Bach LA, Leeding KS** 2002 Insulin-like growth factors decrease catecholamine content in PC12 rat pheochromocytoma cells. Horm Metab Res 34:487–491
31. **Shin SI, Freedman VH, Risser R, Pollack R** 1975 Tumorigenicity of virus-transformed cells in nude mice is correlated specifically with anchorage independent growth in vitro. Proc Natl Acad Sci USA 72:4435–4439
32. **Dahmer MK, Ji L, Perlman RL** 1989 Characterization of insulin-like growth factor-I receptors in PC12 pheochromocytoma cells and bovine adrenal medulla. J Neurochem 53:1036–1042
33. **Dahmer MK, Hart PM, Perlman RL** 1990 Studies on the effect of insulin-like growth factor-I on catecholamine secretion from chromaffin cells. J Neurochem 54:931–936
34. **Frödin M, Gammeltoft S** 1994 Insulin-like growth factors act synergistically with basic fibroblast growth factor and nerve growth factor to promote chromaffin cell proliferation. Proc Natl Acad Sci USA 91:1771–1775
35. **Hanahan D, Weinberg RA** 2000 The hallmarks of cancer. Cell 100: 57–70
36. **Sell C, Rubini M, Rubin R, Liu JP, Efstratiadis A, Baserga R** 1993 Simian virus 40 large tumor antigen is unable to transform mouse embryonic fibroblasts lacking type 1 insulin-like growth factor receptor. Proc Natl Acad Sci USA 90:11217–11221
37. **Jones RA, Campbell CI, Gunther EJ, Chodosh LA, Petrik JJ, Khokha R, Moorehead RA** 2007 Transgenic overexpression of IGF-IR disrupts mammary ductal morphogenesis and induces tumor formation. Oncogene 26:1636–1644
38. **Kim HJ, Litzenburger BC, Cui X, Delgado DA, Grabiner BC, Lin X, Lewis MT, Gottardis MM, Wong TW, Attar RM, Carboni JM, Lee AV** 2007 Constitutively active type I insulin-like growth factor receptor causes transformation and xenograft growth of immortalized mammary epithelial cells and is accompanied by an epithelial-to-mesenchymal transition mediated by NF-κB and snail. Mol Cell Biol 27:3165–3175
39. **Plymate SS, Bae VL, Maddison L, Quinn LS, Ware JL** 1997 Type-1 insulin-like growth factor receptor reexpression in the malignant phenotype of SV40-T-immortalized human prostate epithelial cells enhances apoptosis. Endocrine 7:119–124
40. **Sutherland BW, Knoblaugh SE, Kaplan-Lefko PJ, Wang F, Holzenberger M, Greenberg NM** 2008 Conditional deletion of insulin-like growth factor-I receptor in prostate epithelium. Cancer Res 68: 3495–3504
41. **Zhang M, Hu Z, Huang J, Shu Y, Dai J, Jin G, Tang R, Dong J, Chen Y, Xu L, Huang X, Shen H** 2010 A 3′-untranslated region polymorphism in IGF1 predicts survival of non-small cell lung cancer in a Chinese population. Clin Cancer Res 16:1236–1244
42. **Anzo M, Cobb LJ, Hwang DL, Mehta H, Said JW, Yakar S, LeRoith D, Cohen P** 2008 Targeted deletion of hepatic Igf1 in TRAMP mice leads to dramatic alterations in the circulating insulin-like growth factor axis but does not reduce tumor progression. Cancer Res 68: 3342–3349
43. **Moore T, Carbajal S, Beltran L, Perkins SN, Yakar S, Leroith D, Hursting SD, Digiovanni J** 2008 Reduced susceptibility to two-stage skin carcinogenesis in mice with low circulating insulin-like growth factor I levels. Cancer Res 68:3680–3688
44. **Wu Y, Cui K, Miyoshi K, Hennighausen L, Green JE, Setser J, LeRoith D, Yakar S** 2003 Reduced circulating insulin-like growth factor I levels delay the onset of chemically and genetically induced mammary tumors. Cancer Res 63:4384–4388
45. **Yakar S, Liu JL, Fernandez AM, Wu Y, Schally AV, Frystyk J, Chernausek SD, Mejia W, Le Roith D** 2001 Liver-specific igf-1 gene deletion leads to muscle insulin insensitivity. Diabetes 50:1110–1118
46. **Yakar S, Setser J, Zhao H, Stannard B, Haluzik M, Glatt V, Bouxsein ML, Kopchick JJ, LeRoith D** 2004 Inhibition of growth hormone action improves insulin sensitivity in liver IGF-1-deficient mice. J Clin Invest 113:96–105
47. **Kamio T, Shigematsu K, Kawai K, Tsuchiyama H** 1991 Immunoreactivity and receptor expression of insulinlike growth factor I and insulin in human adrenal tumors. An immunohistochemical study of 94 cases. Am J Pathol 138:83–91
48. **Mertani HC, Delehaye-Zervas MC, Martini JF, Postel-Vinay MC, Morel G** 1995 Localization of growth hormone receptor messenger RNA in human tissues. Endocrine 3:135–142
49. **Maeda K, Chung YS, Ogawa Y, Takatsuka S, Kang SM, Ogawa M, Sawada T, Sowa M** 1996 Prognostic value of vascular endothelial growth factor expression in gastric carcinoma. Cancer 77:858–863
50. **Toi M, Kondo S, Suzuki H, Yamamoto Y, Inada K, Imazawa T, Taniguchi T, Tominaga T** 1996 Quantitative analysis of vascular endothelial growth factor in primary breast cancer. Cancer 77: 1101–1106
51. **Miele C, Rochford JJ, Filippa N, Giorgetti-Peraldi S, Van Obberghen E** 2000 Insulin and insulin-like growth factor-I induce vascular endothelial growth factor mRNA expression via different signaling pathways. J Biol Chem 275:21695–21702